COB09-1316 - DYNAMIC MODELING, SIMULATION AND CONTROL OF AN AUTONOMOUS QUADCOPTER AIRCRAFT

Rafael Fernandes de Oliveira, rafael.fernandes.oliveira@usp.br, rafael.usp@gmail.com
Department of Material, Automotive and Aeronautical Engineering, Engineering School of São Carlos, University of São Paulo
Av. Trabalhador São-carlense, 400, Pq Arnold Schimidt - São Carlos – SP - Brazil, CEP 13566-59

Fábio Toledo Bonemer de Salvi, fabiodesalvi@yahoo.com.br
Department of Material, Automotive and Aeronautical Engineering, Engineering School of São Carlos, University of São Paulo
Av. Trabalhador São-carlense, 400, Pq Arnold Schimidt - São Carlos – SP - Brazil, CEP 13566-59

Eduardo Morgado Belo, belo@sc.usp.br
Department of Material, Automotive and Aeronautical Engineering, Engineering School of São Carlos, University of São Paulo
Av. Trabalhador São-carlense, 400, Pq Arnold Schimidt - São Carlos – SP - Brazil, CEP 13566-59

Abstract. *The use of autonomous aircrafts for inspection tasks has increased in the last years, and while small conventional aircrafts and helicopters have been used with great success, new concepts for autonomous aircrafts have been proposed. The quadcopter platform is one of these, and consists of two pairs of rotors with opposite rotation, installed in a cross-like structure. It is capable of hovering and tracking waypoints with improved stability, guaranteed by the presence of high-frequency controllers with feedback from gyroscopes, accelerometers and magnetometers. This is what makes the quadcopter platform to perform imaging tasks with higher quality. This work describes the development of a full autonomous quadcopter platform, describing its structural and electrical project, the development of a simulation environment using The Mathworks® Matlab & Simulink package, the creation of a hierarchical control based on cascaded PIDs, and the proposed test-bed of the platform using hardware-in-the-loop approach.*

Keywords: *Quadcopter, Aircraft Design, Aerial Robotic, Simulation, Aeronautical Engineering*

1. INTRODUCTION

The current project was proposed during a research for autonomous aircrafts in the Unmanned Aircraft Vehicles (*UAV*) Research Team of University of São Paulo. The need of high image quality and stability proposed by oil and electrical companies drove the requirements for the new autonomous system. The classical solution, of using small model helicopters, was discarded due to the high complexity of the complete system (with many moving parts, and fast dynamics), and a simpler, but not less capable, solution was found in the use of an autonomous quadcopter aircraft.

The quad rotor is an excellent flying platform for studying automatic control, trajectory planning and collision avoidance. Since the quad rotor is dynamically unstable, control algorithms are required for stabilization.

These aircraft have a very simple composition, mainly constructed of four or more rotors, associated with a light structure made of aluminum or carbon fiber, and an embedded control system, responsible to stabilize the aircraft and to allow directional control. The proposed platform has a requirement of at least half an hour of flight time, and with the evolution of batteries, larger flight times are expected in the future.

This paper describes the work done in the area of simulating this quadcopter platform, which allowed the creation of a laboratory environment where the control algorithms could be tested before been embedded in the real aircraft. The simulation was made with the use of the commercial package *Matlab/Simulink*, which was chosen because the hardware of the platform, composed of a 16 bits *dsPIC* microprocessor, can receive the compiled code directly from the simulation environment of Matlab/Simulink.

2. QUADCOPTER DESIGN

The mechanical design of the proposed aircraft consists mainly of four electrical motors and its rotors, a battery pack, a microprocessor capable of running the control algorithms, and a very light structure, made of aeronautical aluminum and carbon fiber tubes.

Figure 1 - Quadcopter Platform

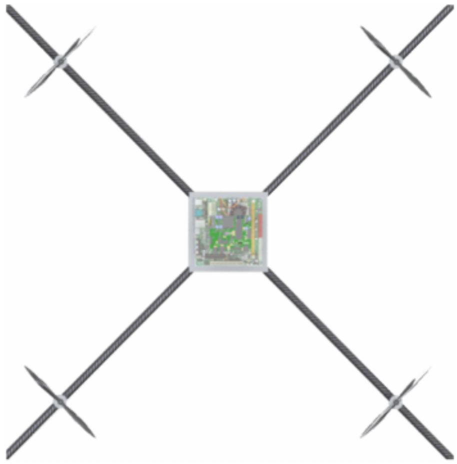

Figure 2 – Top overview of the quadcopter platform

The motors, selected from commercially available brushless-sensorless electric motors, are four *DualSky XM2830CA-12*, with electronic speed controllers *DualSky XC2512BA*. The main characteristics of these components are detailed in Table 1.

Table 1 - Motor and Controller Characteristics

Controller	Max. Continuous Output	Max Peak Output	Weight	Size
XC2512BA	25 A	35 A	22 g	47 x 26 x 7 mm

Motor	Max. Efficiency Current	Max. Input Power 15 s	Weight	KV
XM2830-CA	13 A	200 W	55 g	980 RPM/V

Figure 3 - Speed Control and Brushless Motor

These motors were chosen because of their high Power to Weight Ratio, and were tested in an open circuit wind-tunnel to get the effects of frontal wind in the thrust performance, giving the PWM signal to Force graph shown in Figure 4. A maximum thrust of 6.1 N was achieved in static tests, and 4.5 N with 9.8 m/s frontal wind, using an APC propeller with 10 inches of diameter and 4.8 inches of pitch. A requirement of the propellers is the need of tractor and pusher availability with similar performance.

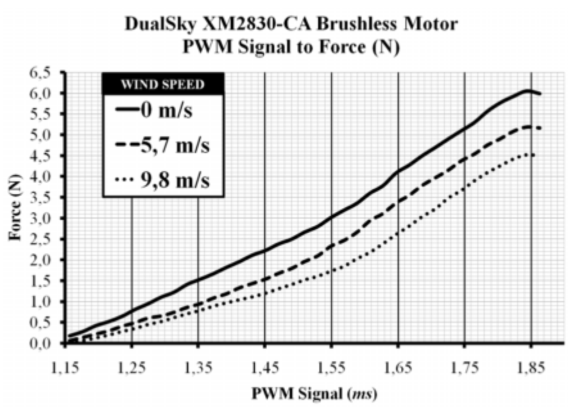

Figure 4 - *DualSky XM2830-CA* Thrust Curves measured in Open Circuit Wind Tunnel

2. MODELING THE QUADCOPTER

Traditional helicopters control its flight by varying the collective pitch of the rotor blades, thought the use of a mechanical device known as a swash plate to change the pitch angle of the rotor blades in a cyclic manner, allowing for pitch and roll control of the vehicle. In contrast, the quad rotor has four constant pitch blades, and is controlled by varying the angular speed of each rotor. The force produced by each motor is proportional to the square of its angular speed. Since each motor turns in the same direction, the produced force is always positive. To cancel gyroscopic effects, two opposite motors rotate clockwise, while the other two rotate counterclockwise.

The difference between the front and the rear rotor angular speed allows for pitch control, while roll control is obtained similarly. The yaw control is created by reducing the angular speed in the clockwise motors, and increasing in the others (or vice-versa). In trimmed flight the sum of the torques is in such way that they tend to cancel each other. The main thrust is the sum of the individual thrusts of each motor.

In body coordinates, we have:

$$F_{3x1} = \begin{bmatrix} 0 \\ 0 \\ 1 \end{bmatrix} \cdot \sum_{i=1}^{4} F_i - \begin{bmatrix} 0 \\ 0 \\ W \end{bmatrix} \cdot D_{\substack{ECEF \\ to\ Body}}$$

$$M_{3x1} = \begin{bmatrix} (F_1 + F_2) - (F_3 + F_4) \\ (F_1 + F_4) - (F_2 + F_3) \\ 0 \end{bmatrix} \cdot l + \begin{bmatrix} 0 \\ 0 \\ \left(\sqrt{\frac{F_1}{K}} + \sqrt{\frac{F_3}{K}}\right) - \left(\sqrt{\frac{F_2}{K}} + \sqrt{\frac{F_4}{K}}\right) \end{bmatrix}$$

Where:

- $\mathbf{F_i}$ is the thrust of the i^{th} motor.
- **W** is the weight of the platform.
- **D** is the direct cosine matrix for translating Earth-Center, Earth-Fixed Coordinates to Body Coordinates.
- **K** is the experimental conversion factor between angular rotation and force

These forces are used as input for the six degree of freedom coordinate system, fixed in both origin and orientation to the moving quadcopter, which is assumed to be rigid:

- The *x*-axis and y-axis are perpendicular to each other and points through each pair of rotors.
- The *z*-axis points down through the bottom of the quadcopter, perpendicular to the *x*-*y* plane.
- The three rotational degrees of freedom are defined by the Euler angles Φ, Θ, Ψ. They are
- Φ: Roll about the *x*-axis
- Θ: Pitch about the *y*-axis
- Ψ: Yaw about the *z*-axis

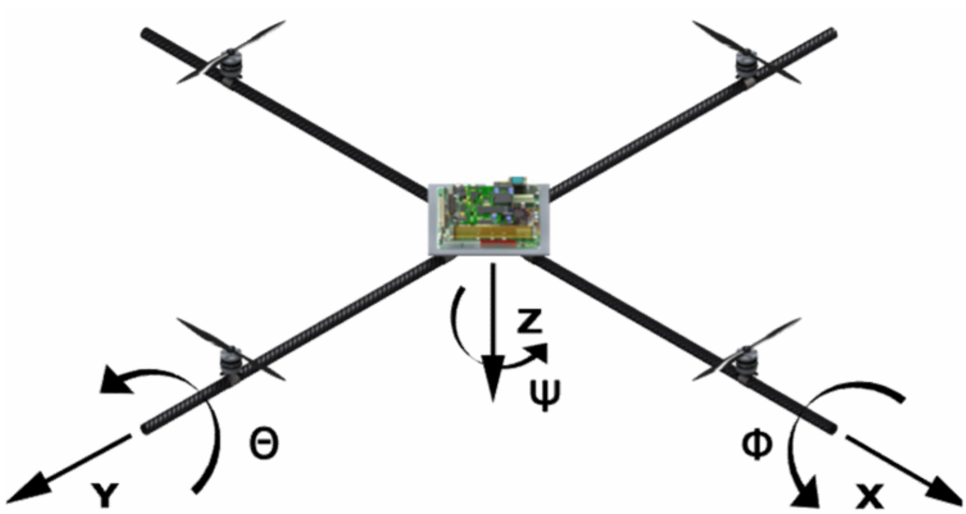

Figure 5 - Body fixed coordinate system

2.1 Sensors Input and Modeling

The sensors available to the embedded control were chosen between commercial Micro-electro-mechanical Sensors (*MEMS)*, such as Magnetometers, Accelerometers, Gyroscopes and Pressure Sensors.

In order to improve the fidelity of the simulation, a model of the noise of each sensor that will be embedded in the quadcopter was created, by summing a random white noise with power proportional to the measured mean value of commercial *MEMS* sensors that were chosen to this platform.

Table 2 - Sensor Data

Sensor	Type	Range	Average Noise
MicroMag3	3-Axis Magnetometer	+/- 1100 μT	0.015 μT
ADXRS150	Z Gyroscope	+/- 150 °/s	0.05°/s/Hz
MMA1250	Z Accelerometer	5 g	0.005 g

2.2 Stabilization and Control

In order to archive trimmed flight, the quadcopter aircraft must have a highly responsive control system, able to reject noises from the sensors, and capable of hovering while maintaining the craft attitude. In order to achieve this, the control system was divided into two main loops: The inner loop is responsible to maintain the attitude and altitude of the quadcopter, and is run in pace with the sensors acquisition rate. The outer loop generate the attitude control inputs required to track a determined waypoint in the X-Y plane, and is run in pace with the signals from the Global Positioning System (GPS) module.

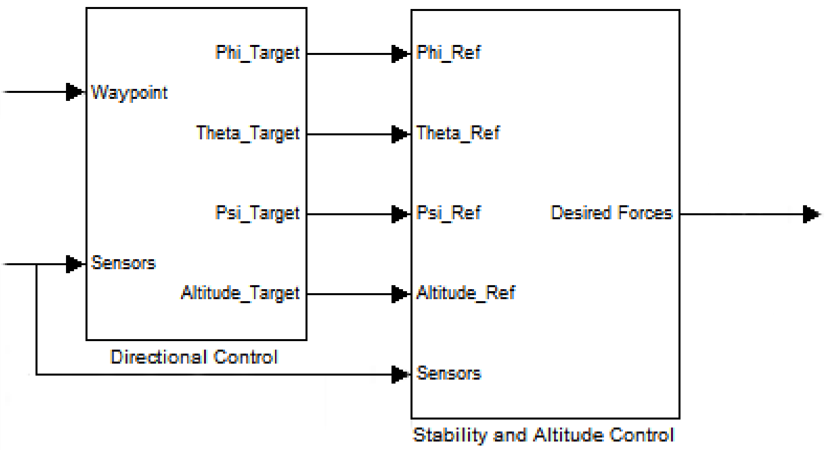

Figure 6 – Cascaded PID controller

Both loops are made of Proportional, Derivative and Integrative (PID) controls.

2.3 Attitude and Altitude Stabilization

The Attitude and Altitude Stabilization System is composed of *PIDs* that are responsible of keeping the quadcopter in a desired angular state, while keeping its altitude. The outputs of this part of the control are linked directly to the rotor angular speed, and their inputs came from the outer control loop, and are composed of the desired Euler angles (Φ, Θ and Ψ). The input of each PID is the error between the desired and the actual signal, as described above.

$$\Phi_{Error} = \Phi_{Control} - \Phi_{Sensors}$$
$$\Theta_{Error} = \Theta_{Control} - \Theta_{Sensors}$$
$$\Psi_{Error} = \Psi_{Control} - \Psi_{Sensors}$$
$$\delta_{\Phi} = K_{P_\Phi} \cdot \Phi_{Error} + K_{I_\Phi} \cdot \int \Phi_{Error}\, dt + K_{D_\Phi} \cdot \frac{d}{dt}\Phi_{Error}$$

$$\delta_{\Theta} = K_{P_\Theta} \cdot \Theta_{Error} + K_{I_\Theta} \cdot \int \Theta_{Error}\, dt + K_{D_\Theta} \cdot \frac{d}{dt}\Theta_{Error}$$

$$\delta_{\Psi} = K_{P_\Psi} \cdot \Psi_{Error} + K_{I_\Psi} \cdot \int \Psi_{Error}\, dt + K_{D_\Psi} \cdot \frac{d}{dt}\Psi_{Error}$$

In order to improve the dynamic response of the controller, additional terms based on the angular velocity were also incorporated in the stabilization loop, in such way that the desired response is quasi-steady state, with near zero angular velocity. In order to obtain this, another PID loop is added to the system, as described above.

$$\dot{\Phi}_{Error} = -\dot{\Phi}_{Sensors}$$

$$\dot{\Theta}_{Error} = -\dot{\Theta}_{Sensors}$$

$$\dot{\Psi}_{Error} = -\dot{\Psi}_{Sensors}$$

$$\delta_{\dot{\Phi}} = K_{P_{\dot{\Phi}}} \cdot \dot{\Phi}_{Error} + K_{I_{\dot{\Phi}}} \cdot \int \dot{\Phi}_{Error}\, dt + K_{D_{\dot{\Phi}}} \cdot \frac{d}{dt}\dot{\Phi}_{Error}$$

$$\delta_{\dot{\Theta}} = K_{P_{\dot{\Theta}}} \cdot \dot{\Theta}_{Error} + K_{I_{\dot{\Theta}}} \cdot \int \dot{\Theta}_{Error}\, dt + K_{D_{\dot{\Theta}}} \cdot \frac{d}{dt}\dot{\Theta}_{Error}$$

$$\delta_{\dot{\Psi}} = K_{P_{\dot{\Psi}}} \cdot \dot{\Psi}_{Error} + K_{I_{\dot{\Psi}}} \cdot \int \dot{\Psi}_{Error}\, dt + K_{D_{\dot{\Psi}}} \cdot \frac{d}{dt}\dot{\Psi}_{Error}$$

In order to maintain the altitude of the quadcopter, a term related to the error between the desired altitude and the one defined by each waypoint is multiplied by the quadcopter weight and used as part of the desired forces, so that the aircraft is capable of hovering without the need of errors in altitude to compensate the weight.

$$H_{Error} = H_{Control} - H_{Sensors}$$

$$\delta_{H} = \left[\left(K_{P_H} \cdot H_{Error} + K_{I_H} \cdot \int H_{Error}\, dt + K_{D_H} \cdot \frac{d}{dt}H_{Error}\right) + 1\right] \cdot (mass \cdot g)$$

In a similar way, the altitude control wanted response is quasi-steady state, with near zero vertical velocity. So the following PID loop is added to the control.

$$\dot{H}_{Error} = -\dot{H}_{Sensors}$$

$$\delta_{\dot{H}} = K_{P_{\dot{H}}} \cdot \dot{H}_{Error} + K_{I_{\dot{H}}} \cdot \int \dot{H}_{Error}\, dt + K_{D_{\dot{H}}} \cdot \frac{d}{dt}\dot{H}_{Error}$$

The desired forces in each rotor are then function of these parameters:

$$F_1 = \delta_{\Phi} + \delta_{\Theta} + \delta_{\Psi} + \delta_{\dot{\Phi}} + \delta_{\dot{\Theta}} + \delta_{\dot{\Psi}} + \delta_{H} + \delta_{\dot{H}}$$

$$F_2 = \delta_{\Phi} - \delta_{\Theta} - \delta_{\Psi} + \delta_{\dot{\Phi}} - \delta_{\dot{\Theta}} - \delta_{\dot{\Psi}} + \delta_{H} + \delta_{\dot{H}}$$

$$F_3 = -\delta_{\Phi} - \delta_{\Theta} + \delta_{\Psi} - \delta_{\dot{\Phi}} - \delta_{\dot{\Theta}} + \delta_{\dot{\Psi}} + \delta_{H} + \delta_{\dot{H}}$$

$$F_4 = -\delta_{\Phi} + \delta_{\Theta} - \delta_{\Psi} - \delta_{\dot{\Phi}} + \delta_{\dot{\Theta}} - \delta_{\dot{\Psi}} + \delta_{H} + \delta_{\dot{H}}$$

These forces are then converted to angular velocities, and sent to the controller of each motor, after imposing saturation over the working range of each rotor.

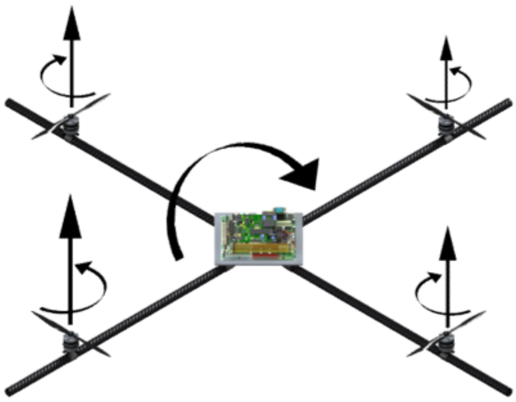

Figure 7 - Pitch Control

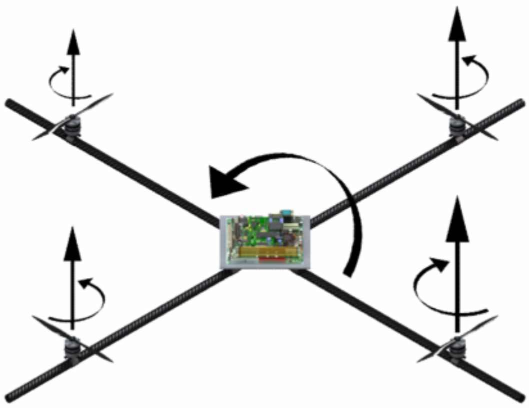

Figure 8 - Row Control

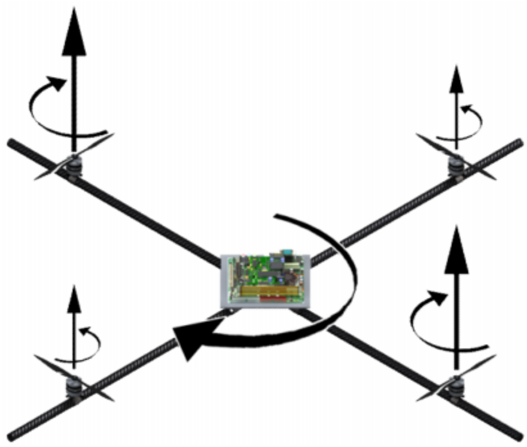

Figure 9 - Yaw Control

2.4 DIRECTIONAL CONTROL

The directional control of the quadcopter is what makes the aircraft autonomous. It is responsible of generating the attitude control signals that will move the quadcopter from the current position to the desired waypoint. This loop consists of four PIDs, connected in such way that their inputs are the projected position error vector in the X and Y axis of the body coordinates.

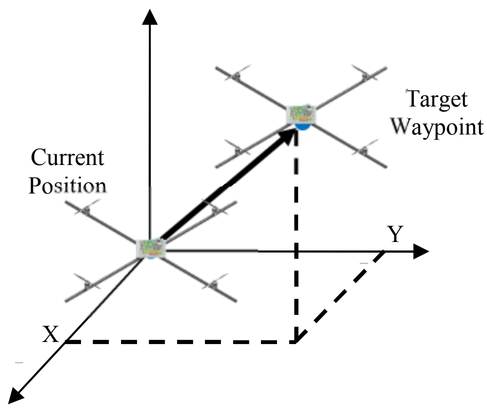

Figure 10 – Waypoint tracking model

$$X_{Error} = X_{Control} - X_{Sensors}$$
$$\delta_X = K_{P_X} \cdot X_{Error} + K_{I_X} \cdot \int X_{Error}\, dt + K_{D_X} \cdot \frac{d}{dt} X_{Error}$$
$$\dot{X}_{Error} = -\dot{X}_{Sensors}$$
$$\delta_{\dot{X}} = K_{P_{\dot{X}}} \cdot \dot{X}_{Error} + K_{I_{\dot{X}}} \cdot \int \dot{X}_{Error}\, dt + K_{D_{\dot{X}}} \cdot \frac{d}{dt} \dot{X}_{Error}$$
$$\Theta_{Control} = \delta_X + \delta_{\dot{X}}$$

$$Y_{Error} = Y_{Control} - Y_{Sensors}$$
$$\delta_Y = K_{P_Y} \cdot Y_{Error} + K_{I_Y} \cdot \int Y_{Error}\, dt + K_{D_Y} \cdot \frac{d}{dt} Y_{Error}$$
$$\dot{Y}_{Error} = -\dot{Y}_{Sensors}$$
$$\delta_{\dot{Y}} = K_{P_{\dot{Y}}} \cdot \dot{Y}_{Error} + K_{I_{\dot{Y}}} \cdot \int \dot{Y}_{Error}\, dt + K_{D_{\dot{Y}}} \cdot \frac{d}{dt} \dot{Y}_{Error}$$
$$\Phi_{Control} = \delta_Y + \delta_{\dot{Y}}$$

3. SIMULATION RESULTS

First, a simulation of the inner control loop was made, so the gains of this part of the control system could be tuned in order to obtain the desired response, without excessive overshoot or oscillation. After the tuning of the inner loop, a simulation of the outer loop was made, in order to tune its gains, with the requirement of no overshoot and as little as possible oscillation. The results of this latter simulation are shown next, in Figure 11

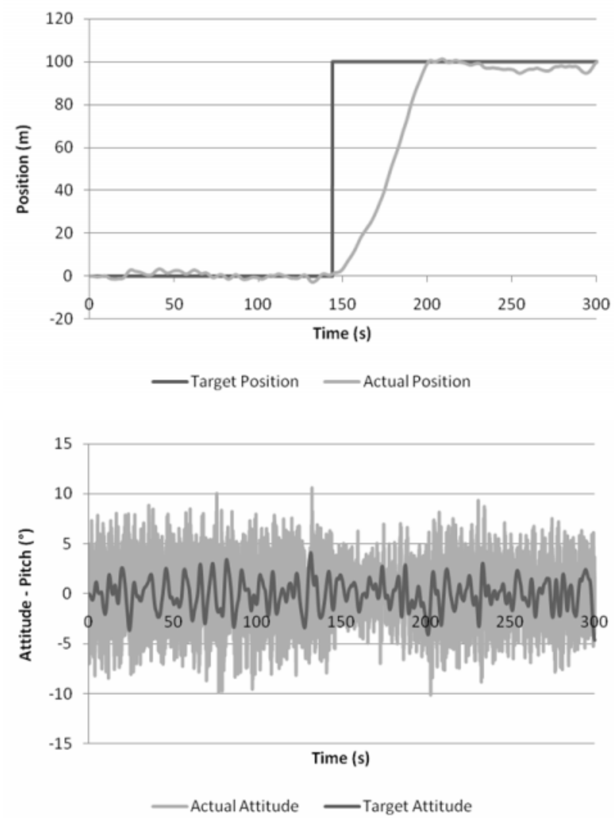

Figure 11 - Hovering Performance

The effect of the noise in the sensors input was then studied, and it was found that the response of the derivative part of the PID control was causing the control to fail. In order to prevent this, a low-pass filter was inserted before the derivative operation of each PID, as shown in Figure 12.

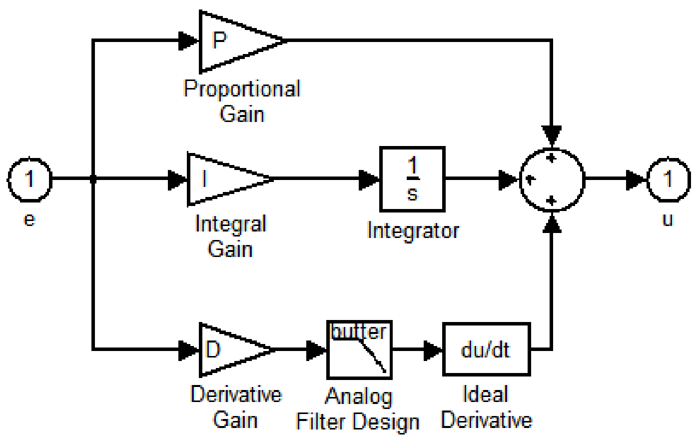

Figure 12 - Modification of the PID Derivative Control

With this, and a little modification in the values of the gains, the simulation was able to handle the noises without loss of control.

4. HARDWARE IMPLEMENTATION

The initial goal of this project was the implementation of the developed control system in an embedded hardware, model *Flexboard* from *Evidence SRL*. This board consists of a RISC microprocessor from Microchip (dsPIC33F256MC710), running at 8MHz, capable of scaling the clock up or down by the use of Phase-locked loop, up to 40MHz. The board has also connections for two RS232 serial ports that are used for receiving data from the GPS system, and to communicate over a radio-link with the ground control, and two Serial Peripheral Interface (SPI) bus, used for connection with a high precision Analog to Digital converter, and with a 3-axis magnetometer.

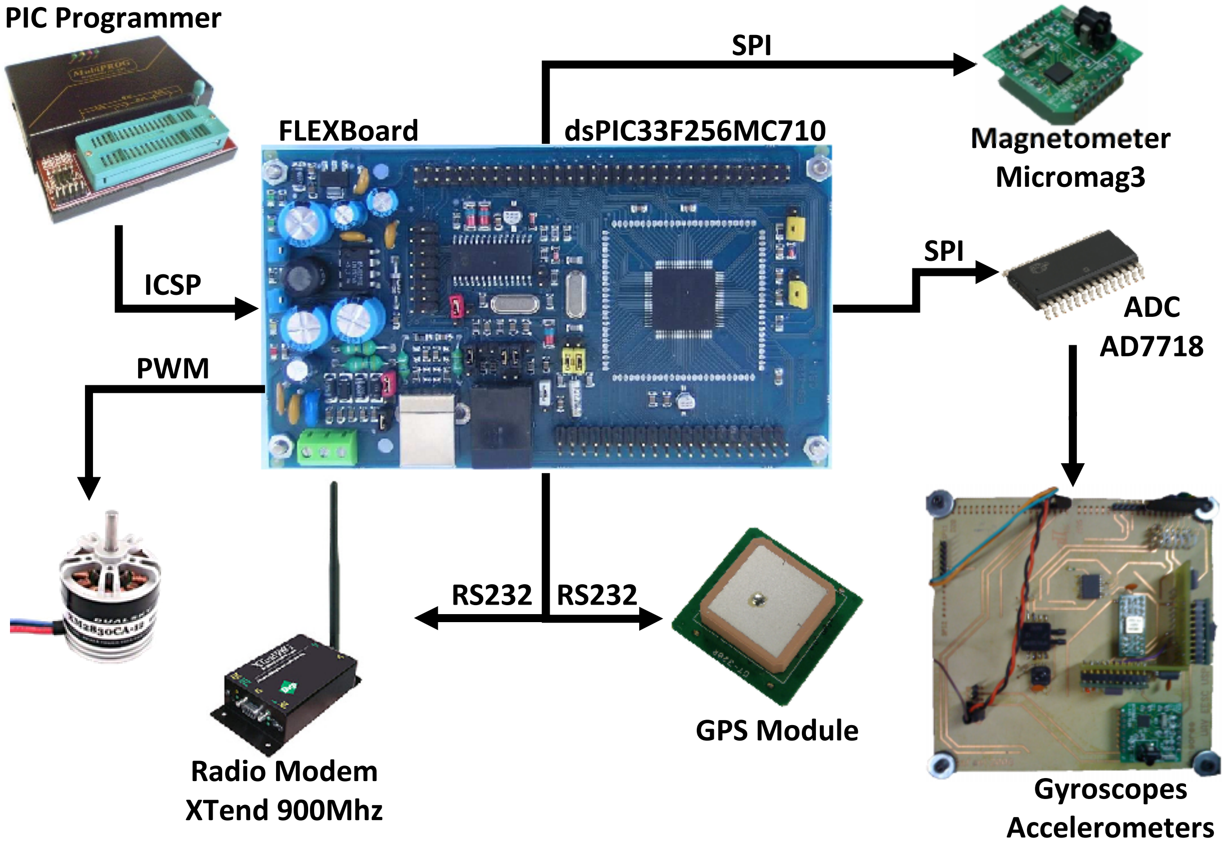

Figure 13 – Schematic of Quadcopter Embedded Hardware

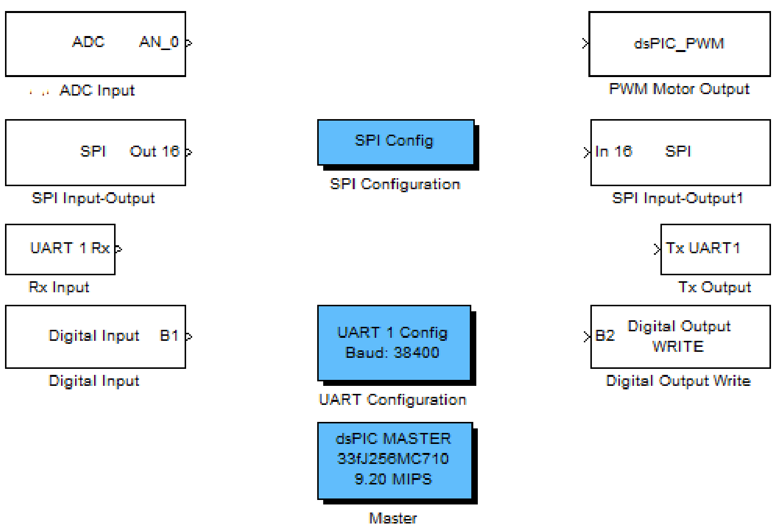

Figure 14 – dsPIC Blockset used for communication with sensors, Radio Modem and GPS. (Kerhuel, 2009)

Using a specific Simulink target, developed for direct compilation of Simulink code to dsPIC compatible code, and with little modification of the main simulation structure, it was possible to port the attitude stabilization loop to the embedded board. The sensor inputs are first filtered using a Kalman Filter, and the desired forces in each motor are converted through a lookup table into a PWM signal that is sent to the controller of the brushless motors.

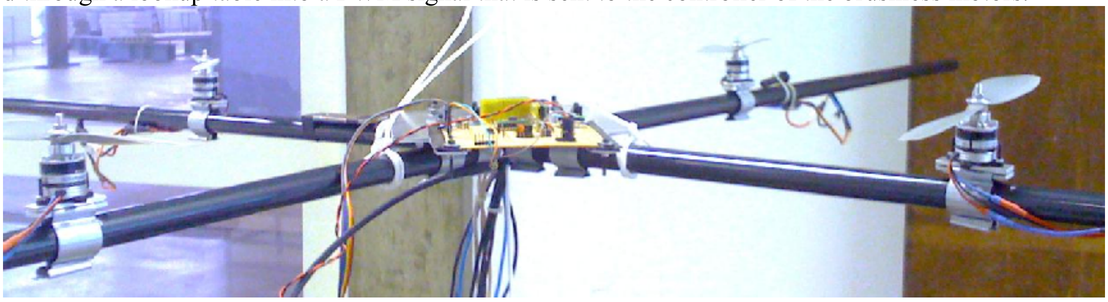

Figure 15 - Quadcopter Platform mounted in university laboratory

5. CONCLUSION

In this paper, a simulation of an autonomous quadcopter aircraft is presented. This simulation focused in having a good representation of the dynamic of the aircraft, modeling forces and moments acting in the platform, and allowed the development of a control algorithm based on two main loops, a inner, responsible of controlling the attitude and altitude, and an outer loop, responsible for the directional control of the quadcopter. The results of the simulation allowed tuning the gains of each PID controller, and after the insertion of random noise in the sensor model, to tune the cut-off frequency of the derivative part of the PID controller.

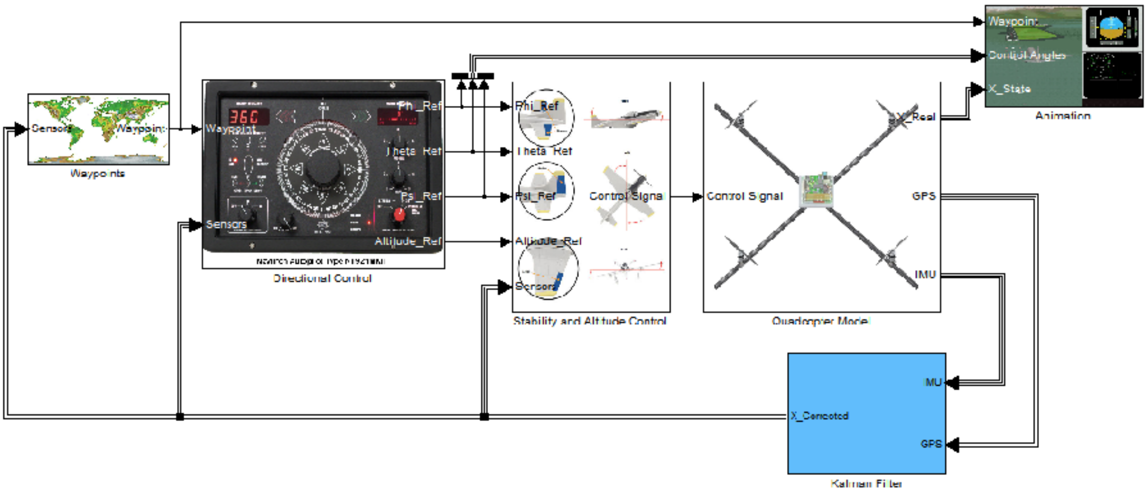

Figure 16 - Simulink® block diagram of the Quadcopter Simulation and Control System

In the future, a more detailed study will be done in order to test different control techniques, such as LQR and Fuzzy. As the control algorithm can be ported directly to the embedded hardware, the simulation will be extended to allow a hardware-in-the-loop simulation with the real microcontroller and structure.

6. REFERENCES

Castillo, P., Lozano, R., & Dzul, A. (2005). Stabilization of a Mini Rotorcraft with Four Rotors.
Corp., T. M. *Matlab/Simulink.*
Evidence SRL. (2009). FLEX Base Boards Datasheet. Pisa, Italy.
Jason, E., Nichols, R., Kitchel, G., Walsh, C., & Welch, J. *Autonomous Quadcopter.*
Kerhuel, L. (2009). Embedded Target for PIC.
Martínez, V. (2007). *Modelling of the Flight Dynamics of a Quadrotor Helicopter.* Cranfield University, Department of Aerospace Sciences.

7. RESPONSIBILITY NOTICE

The authors are the only responsible for the printed material included in this paper.